Microsc. Microanal. Microstruct. 7 (1996) 185–193 JUNE **1996**, PAGE 185

Classification
Physics Abstracts
81.05.Bx — 81.30.Mh — 82.65.Dp

Concentration Gradients near Heterophase Boundaries in Crept Single Crystal Nickel Base Superalloys

Didier Blavette ([1,*]), Laurence Letellier ([1]), Anne Racine ([2]) and Alain Hazotte ([2,**])

([1]) Laboratoire de Microscopie ionique, URA CNRS 808, Université de Rouen, UFR des Sciences et Techniques, 76821 Mont Saint Aignan Cedex, France
([2]) Laboratoire de Science et Génie des Matériaux Métalliques, URA CNRS 159, École des Mines, Parc de Saurupt, 54042 Nancy Cedex, France

(Received May 14; accepted September 24, 1996)

Résumé. — Cet article présente les résultats de l'analyse par sonde atomique des interfaces γ/γ' dans un superalliage monocristallin à base de nickel flué pendant 5 h à 1050 °C, sous une charge uniaxiale de compression de 100 MPa appliquée selon un axe ⟨001⟩. Des variations subtiles de composition sont détectées entre les deux types d'interfaces, parallèles ou perpendiculaires à la direction de la charge. Elles sont interprétées comme les prémices de l'évolution morphologique des précipités conduisant à la "mise en radeaux". La force motrice qui régit la migration des espèces chimiques est discutée grâce à la connaissance du champ de contraintes local obtenu par un calcul aux éléments finis.

Abstract. — This paper presents the results of an atom-probe analysis of γ/γ' interfaces in a nickel base superalloy single crystal which was crept for 5 h at 1050 °C, under a 100 MPa compression stress applied along one ⟨001⟩ direction. Subtle chemistry variations are detected near the two types of interfaces, namely parallel and perpendicular to the stress direction. They are interpreted as evidence for the early stage of precipitate shape evolution as the origin of "rafting". The driving force for migration of solute elements is discussed in the light of local stress field calculations using finite element modelling.

1. Introduction

Oriented coarsening has been observed for more than thirty years in both polycrystal and single crystal two-phase materials [1-5]. This phenomenon is of upmost importance in nickel base superalloys as it controls the creep performance of these materials at high temperatures. Single crystal alloys are developed for blades of engine turbines and owe their excellent creep performances, at temperatures exceeding 1000 °C, to the presence of a high volume fraction of ordered

(*) also at the Institut Universitaire de France
(**) Author for correspondence

γ' precipitates ($L1_2$-Ni_3Al type). Under stress, γ' particles are observed to coarsen in the form of γ' rafts whose orientation depends on both the stress direction and the value of coherency misfit between γ matrix and γ' particles. In the case of a tensile stress along the $\langle 001 \rangle$ direction, rafts develop perpendicular to the stress axis for negative values of the misfit parameter δ ($\delta = 2(a_{\gamma'} - a_\gamma)/(a_{\gamma'} + a_\gamma)$, with a_γ and $a_{\gamma'}$ the lattice parameters of γ and γ' phases, respectively), and parallel for positive values. In the case of a compressive stress, the evolution is reversed [5-7]. Clearly, the driving force for oriented coarsening is a combination of coherency misfit internal stresses and applied stress.

Although oriented coarsening in two-phase single-crystal superalloys has been widely studied during the last two decades, few data related to the thermodynamic stability of interfaces in crept materials are available [8, 9]. One of the main difficulties is that a very high spatial resolution is needed to get the local compositions in the immediate vicinity of interfaces, typically a single atomic layer. However, this point is a key issue for the in-depth understanding of physical processes driving creep phenomena.

In this paper, atom-probe techniques have been applied to the nanoanalysis of γ/γ' interfaces in a crept single crystal of MC2 superalloy. More details on this latest generation superalloy can be found elsewhere [10]. Because of its high spatial resolution (0.1 nm in depth), the atom-probe is a well suited technique for the investigation of internal interfaces. Compared to other nanoanalytical tools (EELS, EDX), one of its main advantages is its quantitativity [11, 12]. The aim of this study was to understand the influence of an applied stress on the chemical compositions at γ/γ' interfaces. Material was crept along the $\langle 001 \rangle$ direction, at low stress, high temperature and for a short time. Then the local concentrations were investigated near both types of interfaces, namely parallel and perpendicular to the stress axis. The differences observed will be presented and discussed in terms of diffusion mechanisms, in the light of internal stress field calculations using finite element modelling.

2. Experimental

$\langle 001 \rangle$ oriented single crystals of MC2 nickel-based superalloy were supplied by SNECMA. The material was subjected to a three-stage standard heat treatment composed of a homogenization sequence at 1300 °C for 3 h (+Air Cooling) followed by a two-step precipitation annealing (1080 °C/6 h A.C + 870 °C/20 h A.C). This treatment leads to the formation of a high volume fraction (70%) of γ' precipitates with a mean size of about 0.4 μm. Due to elastic anisotropy and lattice mismatch, γ' particles are cuboidal and aligned along $\langle 001 \rangle$ directions. Phase composition and microstructural details may be found in reference [13].

A cylindrical sample (diameter 10 mm; length 15 mm parallel to the $\langle 001 \rangle$ growth axis) was crept along $\langle 001 \rangle$ direction for 5 h, at 1050 °C and under a compressive stress of 100 MPa. Then, the specimen was quenched by argon sweeping (> 2000 °C h^{-1}) in order to prevent solute redistribution between γ and γ' phases during cooling. Only a small amount of very fine γ' particles was observed in some γ corridors after quenching. The misfit of MC2 alloy being negative at high temperature [14,15], this type of creep test would have led to γ' rafting parallel to the stress axis after longer creep times. In the present case, the time was too short to allow a strong structural evolution. The γ' precipitates remained roughly cuboidal, although a slight elongation along the stress axis was detected on average by image analysis [16]. The deformation was observed to be heterogeneous, with large areas free of dislocations, while others showed dislocations preferentially localized in the γ corridors parallel to the stress axis and along the corresponding γ/γ' interfaces (early beginning of mismatch relaxation by dislocation arrays). Note that precipitate elongation was detected either in areas free of dislocations or in areas with dislocations [16].

Table I. — *Matrix composition near N interfaces (C_i^γ) as compared to that at the centre of γ corridors (C_0^γ). The precision is mainly controlled by counting statistics: $\Delta C = 2\sigma$ with $\sigma = \sqrt{C(1-C)/N}$ the standard deviation and N the total number of collected ions.*

	Al	Ti	Ta	Al+Ti+Ta	Ni	Cr	Mo	Co	W
C_i^γ	1.8	0.2	0.1	2.1	58	23	4	9	4
at.%$\pm 2\sigma$	± 0.7	± 0.2	± 0.2	± 0.8	± 3	± 2	± 1	± 1	± 1
$N = 1300$ ions									
C_i^γ	2.8	0.3	0.5	3.6	58	20.9	3.1	10.1	3.8
at.%$\pm 2\sigma$	± 0.3	± 0.1	± 0.1	± 0.4	± 1	± 0.8	± 0.4	± 0.6	± 0.4
$N = 9000$ ions									

Analysis of γ/γ' interface chemical composition was conducted using a conventional atom-probe. This technique combines the possibilities of field ion microscopy with those of a single-atom sensitive time-of-flight mass spectrometer. Samples were cut along $\langle 001 \rangle$ directions parallel and perpendicular to the load axis. They were prepared in the form of sharply pointed needles ($R \cong 50$ nm) in order to be field evaporated by high-voltage pulses. Only ions coming from a small selected region of the tip surface are mass analysed. Layer after layer, depth profiles related to each species are generated. These profiles correspond to the analysis of samples along a direction parallel to the tip axis. The lateral resolution is typically 2 nm. More details can be found elsewhere [11].

3. Results

Depth profiles related to γ/γ' interfaces normal to the stress axis (called hereafter N interfaces) are presented in Figure 1. These clearly show that a Cr-rich and Al-depleted γ corridor 100 nm wide was crossed during analysis. This corridor separates two Al-enriched and Cr-depleted γ' particles. These profiles exhibit the presence of local concentration gradients near γ/γ' interfaces which spread over 20 nm. Aluminium and nickel levels in γ in the immediate vicinity of the boundaries are lower than those observed in the centre of γ corridors. A similar behaviour is observed for other γ'-forming elements such as titanium or tantalum. Opposite gradients are exhibited for chromium which is the main γ-forming element. In Table I, the concentrations averaged over a small region in the close vicinity of the N interface displayed in Figure 1 are compared to those at the center of the γ corridors. Because of statistical fluctuations due to counting errors, no concentration differences are revealed for Ni in Table I. Only a trend along the Ni profile (exhibited by a solid line) can be observed in Figure 1. Due to the small distance over which concentration gradients occur (< 20 nm), the number of ions is limited ($N = 1300$), leading therefore to important statistical fluctuations (in Tab. I, ΔC is taken to be two times the standard deviation). The integration of concentration gradients over a larger distance, in order to ensure better counting statistics, would lead to smaller measured differences between both regions. Clearly, a compromise must be found between depth resolution and accuracy of measurements. The atom-probe data reported in Table I are the result of this compromise. Despite their limited precision, the measurements clearly indicate that the amount of γ'-forming elements (Al, Ti, Ta) is lower near N interface than in the core of γ corridors. Moreover, the concentration gradients displayed in

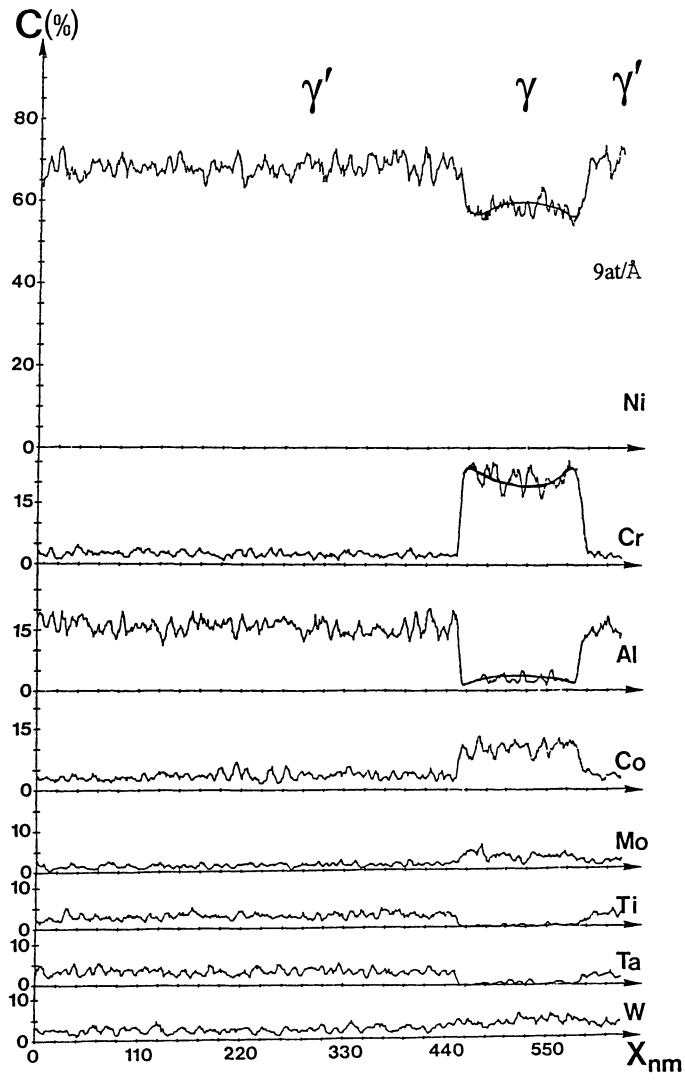

Fig. 1. — Depth profiles related to the analysis of γ/γ' interfaces (N) perpendicular to the stress axis. The direction of analysis is [001] and perpendicular to interface. Depth resolution is close to 0.1 nm. Interfaces are located at the abrupt transitions of Cr and Al profiles. Solid lines are just guides for the reader's eyes.

Figure 1 for Al, Ti and Ta demonstrate unambiguously that local depletions occur near N interfaces. Measured Al, Ti and Ta concentrations gradually increase when approaching the corridor core. The reverse tendency is exhibited for Cr.

Thought more subtle, inverse tendencies were observed near γ/γ' interfaces parallel to the stress axis (called hereafter P interfaces). Such gradients are visible in Figure 2, especially for nickel. These are less evident for chromium and aluminium. Atom-probe analyses did not reveal important average composition differences between P-type and N-type γ corridors.

Very few data are available on the chemistry of γ/γ' interfaces [8, 9] or γ corridors [8, 9, 16, 17] in crept superalloy single crystals. Since all these data were obtained by energy dispersive

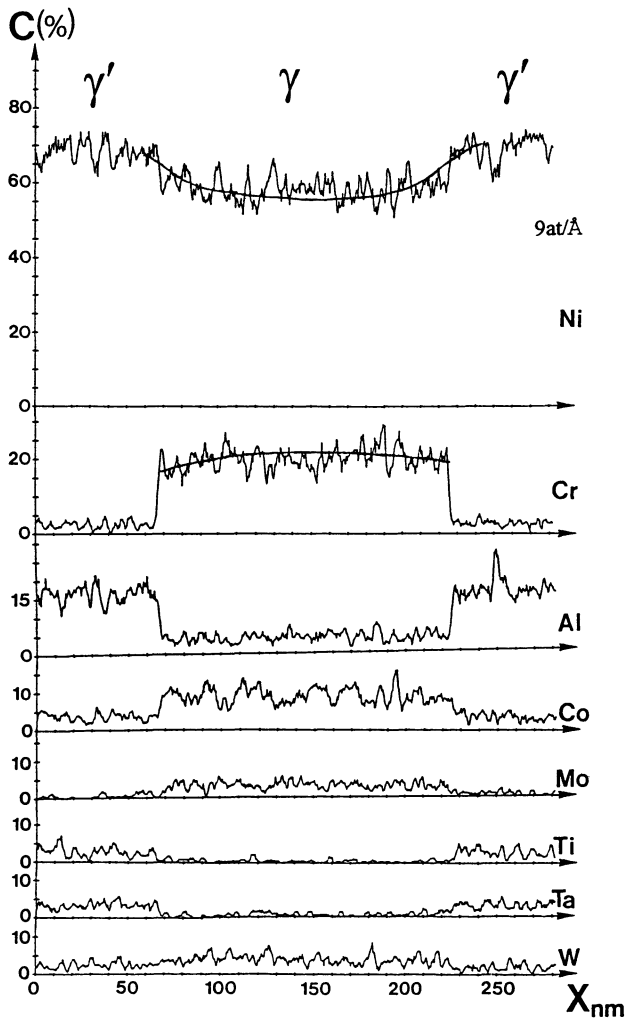

Fig. 2. — Depth profiles related to the analysis of γ/γ' interfaces (P) parallel to the stress axis. The direction of analysis is [010] and perpendicular to interface. Interfaces are located at the abrupt transitions of Cr and Al profiles. Solid lines are just guides for the reader's eyes.

X-ray (EDX) analysis, a quantitative comparison with the present experimental results is difficult. Atom-probe microscopy has a much higher spatial resolution and is therefore particularly reliable in the case of heterophases boundaries, while EDX is subjected to bias due to the larger volume over which concentrations are averaged [9]. Conversely, atom-probe measurements are less representative than EDX when chemical heterogeneities occur over larger scales (for instance the scale of a γ corridor). A second difficulty in comparing data lies in the differences of experimental creep conditions used. Schmidt and Feller-Kniepmeier (SF) [8] and Buffière *et al.* (BCI) [9] analysed γ/γ' interfaces in single-crystals of SRR99 and CMSX-2 alloys, respectively, but they focused on either low-temperature high-stress or high-temperature long-term creep tests. After a tensile creep test at 980 °C, for 41 h under 170 MPa, SF detected a segregation of Cr and slight gradients in W and Ti near the γ/γ' interfaces, but the sense of these gradients did not depend on

the orientation of the interface with respect to the applied stress. However, in the test conditions, γ' precipitates had already strongly evolved towards rafts with interfaces relaxed by dislocation arrays. After a bending test at 1050 °C under about 300 MPa, BCI showed that such arrays are associated with a larger concentration of Cr and Co and a depletion of Ti and Al, which could explain SF's results. For test conditions closer to ours (980 °C, 170 MPa, 41 h, no drastic precipitate shape evolution), FR did not analyse the γ/γ' interface chemistry but they detect no difference of chemical composition between the two types of γ corridors, which is in agreement with our results. However, this observation is not general, since other works showed that the γ corridors which have to disappear during creep were enriched in γ'-forming elements in the early stages of their evolution [9, 16, 17]. As discussed in [16], a study in this field requires the analysis of a large number of corridors to be statistically representative. This was clearly not the case in the present work which is focussed on local compositions near interfaces.

4. Discussion

The local gradients observed near γ/γ' interfaces are thought to be an experimental evidence for diffusion-driven precipitate rafting (evolution toward plates or rods oriented parallel to the stress axis). The observed impoverishment in Al, Ni and Ti near N interfaces as compared to core levels in γ corridors are thought to be the signature of bulk diffusion of γ'-forming elements towards N interfaces. This down-hill migration will promote the migration of both N interfaces on each side of the γ corridor (Fig. 1), leading to the final coagulation of both γ' precipitates. Inverse fluxes are observed for γ-forming elements like Cr. The opposite gradients observed near P interfaces indicate that γ' particles dissolve from these interfaces, thus supplying N interfaces for their migration (Fig. 2). The γ'-forming elements diffuse from P to N interfaces. Reverse migration occurs for chromium. The observed gradients indicate that coarsening kinetics are controlled by bulk diffusion in the γ solid solution and not by interfacial reaction mechanism. The fact that oriented coarsening is observed to be controlled by diffusion in the γ solid solution is not surprising. Dimitrov and Martin clearly demonstrated that mobility is higher in the solid solution than in the ordered γ' phase [18].

It is now well accepted that the stress induced γ' rafting is related to the existence of an anisotropy of stress and strain at the microscopic scale, that is, at the scale of the elementary unit constituted by a precipitate and the surrounding γ matrix (see [19-21] for reviews). This anisotropy has different origins. In the absence of any plastic deformation (elastic regime), it is due to both the difference of elastic moduli and the difference of lattice parameters between phases, which lead to internal coherency stresses. In the early stages of plastic deformation (relaxed regime), an additional effect comes from the preferential relaxation of a given type of γ corridor (N or P, depending on the signs of load and misfit). The local stress/strain distribution resulting from these different effects can be estimated by finite element modelling [20-26]. In the present study, we simulated the compression test at 1050 °C under 100 MPa, using a 3D finite element model and input data which have been presented in detail elsewhere [16, 26]. This allows us to obtain the local distribution of stress and strain within the matrix and the precipitate. In superalloys with a high volume fraction of γ' precipitates, a general result of finite element calculations is that internal coherency stresses are mainly concentrated in the matrix. In the conditions tested here, stresses and strains are rather homogeneous in the embedded γ' phase, while the main mechanical gradients are found between the different γ corridors. This fact is illustrated in Table II which reports values of the three principal stresses, the hydrostatic stress and the equivalent Von Mises stress (deviatoric component) in the middle of N-type and P-type γ corridors. Two types of γ/γ' interface states have been considered for the calculations: i) the "elastic regime" where all the interfaces are coherent ; ii) the "relaxed regime" where the mismatch is relaxed along the

Table II. — *Stresses in N-type and P-type γ corridors in materials compressed along $\langle 001 \rangle$ direction, as predicted by finite element modelling for an applied stress of 100 Mpa and a misfit of −0.3%. The results are given for both elastic and relaxed cases. σ_{hyd} is the hydrostatic stress whereas σ_{equ} is the equivalent Von Mises stress.*

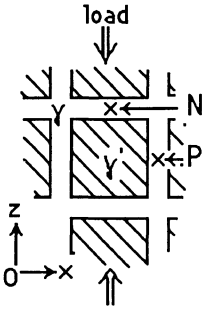

	elastic regime		relaxed regime	
	P	N	P	N
σ_x (MPa)	56	−260	29	−294
σ_y (MPa)	−253	−260	30	−294
σ_z (MPa)	−344	−48	−92	−117
$\sigma_{hyd.}$ (MPa)	−180	−189	−11	−235
$\sigma_{equ.}$ (MPa)	363	212	122	177

two P interfaces parallel to the applied stress. As noted above, these cases correspond to the two extreme situations actually observed in our samples.

From Table II, it is clear that both elastic and relaxed cases are characterised by a high mechanical anisotropy between N and P corridors. It is noted that the strain gradients between γ corridors calculated by finite element modelling is qualitatively confirmed by high-temperature neutron diffraction experiments on similar alloys [15]. Indeed, in the case of compressed samples, these experiments pointed out a strong difference of lattice distortion ("quadraticity") between γ corridors of different orientations. However, the open question is to know how this mechanical anisotropy can induce the chemical rearrangement detected in the present study. Let us recall here that while the equivalent Von Mises stress drives the dislocation movements, it is the hydrostatic stress which is likely to control the local equilibrium concentrations, that is, the chemical potential of each element in the γ solid solution. Table II shows that the N corridors are subjected to the highest hydrostatic stress, whatever the regime considered. Thus, one explanation could be that corridors undergoing more important hydrostatic stresses will be less stable. The stress gradient would promote the diffusion of solutes down the chemical potential gradients thus produced. This diffusion induced by hydrostatic stress gradient has already been proposed by some authors [17, 20]. The major advantage of this model is that it can explain that rafting has been observed in both elastic and relaxed cases — even if it is much slower in the former one. Indeed, the hydrostatic stress component shows the same direction of anisotropy in both regimes, which

is not the case for the deviatoric component. It is noted that this point is only valid if the γ' phase is assumed to be stiffer than the γ phase. If not, the hydrostatic stress anisotropy — therefore the expected raft orientation — would be inverted between elastic and plastic regimes.

It is also interesting to note that the Al depletion near N interfaces should reduce the coherency misfit. As a result, this should minimise the elastic energy stored locally. Aluminium has indeed an atomic radius in the γ phase ($r_{Al} = 0.143$ nm) much larger than that of nickel or chromium (0.124 and 0.127 nm respectively). As $a_\gamma > a_{\gamma'}$ ($\delta < 0$), Al depletion should lead to a slight minimisation of mismatch. Note that this size effect is one of the reasons why the magnitude of δ increases with temperature, thermal expansion being the other. While the γ' composition remains nearly constant with temperature, the solubility in the γ phase of large radii γ'-forming elements such as Al, Ti and Ta increases drastically with temperature [15, 27], leading to an increase of a_γ (a decrease of δ). In industrial alloys similar to MC2, the misfit was found to be positive at room temperature and to become negative at high temperature.

In the ideal case of a coherent binary spherical precipitate embedded in an infinite matrix, Johnson has shown that the application of an external uniaxial load results in a variation of the equilibrium composition along the interface [28], which can be invoked as a possible origin for the difference of chemical compositions measured between the two types of interfaces. It is difficult to argue definitively with regard to the discrepancies between the ideal model and our actual system. However, it is noted that the differences of composition as calculated with Johnson's formulae using data relative to our experimental conditions, are of much lower magnitude than those actually measured in the present study.

5. Conclusion

An atom-probe investigation of the early stages of creep in superalloy MC2 at 1050 °C exhibits the occurrence of concentration gradients near γ/γ' interfaces.

Local depletions of Al, Ta, Ni and Ti, as well as Cr enrichment were detected at heterophase boundaries (N) perpendicular to stress direction. These are observed over a distance close to 20 nm. Opposite gradients are detected in the immediate vicinity of γ/γ' interfaces (P) which are parallel to the deformation axis.

These gradients reveal the nature of diffusion mechanisms under oriented coarsening phenomena: γ'-forming elements generated by the dissolution of P interfaces diffuse towards N interfaces through γ corridors. The migration of N interfaces of two neighbouring γ' particles leads finally to the coagulation of precipitates and thus to the formation of rafts parallel to stress axis. The driving force for migration of solutes is the elastic energy gradient between N and P corridors.

Acknowledgements

This work was supported by the French National Programme "C.P.R. Stabilité Structurale des Superalliages Monocristallins".

References

[1] Webter G.A. and Sullivan P., *J. Inst. Met.* **95** (1967) 138.

[2] Sullivan P., Webter G.A. and Piercey B.J., *J. Inst. Met.* **96** (1968) 274.

[3] Danesi W. and Donachie M., *J. Inst. Met.* **97** (1969) 107.

[4] Tien J.K. and Copley S.M., *Met. Trans.* **2** (1971) 215.
[5] Tien J.K. and Copley S.M., *Met. Trans.* **2** (1971) 543.
[6] Carry C. and Strudel J.L., *Acta metall.* **25** (1977) 767.
[7] Fredholm A., PhD thesis, ENSMP, Paris (1987).
[8] Schmidt R. and Feller-Kniepmeier M., *Scr. Metall. Mater.* **29** (1993) 1079.
[9] Buffiere J.Y., Cheynet M.C. and Ignat M., *Scri. Mater.* **34** (1996) 349.
[10] Caron P. and Khan T., Proc. EUROMAT'89 (Aachen 1989) H.E. Exner, V. Schumacher Eds. (DGM Informationgessellschaft, Oberursel, Germany, 1990) p. 333.
[11] Blavette D. and Menand A., *MRS Bull.* 19, n°7 (1994) 21.
[12] Blavette D., Bostel A., Sarrau J.M., Deconihout B. and Menand A., *Nature* **363** (1993) 432.
[13] Duval S., Chambreland S., Caron P. and Blavette D., *Acta Metall. Mater.* **42** (1994) 185.
[14] Grosdidier T., PhD Thesis, INPL, Nancy (1992).
[15] Royer A., PhD Thesis, Université Joseph-Fourier, Grenoble (1993).
[16] Racine-Kirch A., PhD Thesis, INPL, Nancy (1995).
[17] Svetlov I.L., Golovko B.A., Epishin A.I. and Abalakin N.P., *Scri. Metall. Mater.* **26** (1992) 1353.
[18] Dimitrov O. et Martin G., Proc. Coll. "Superalliages Monocristallins", Toulouse-Seilh, France (pub. SNECMA, 1995) p. 29.
[19] Nabarro F.R.N., *Metall. Mater. Trans. A* **27A** (1996) 213.
[20] Louchet F., Proc. of the Coll. " Superalliages Monocristallins", Toulouse-Seilh, France (pub. SNECMA, 1995) p. 119.
[21] Socrate S. and Parks D.M., *Acta Metall. Mater.* **41** (1993) 2185.
[22] Argon D. and Pollock T.R., Proc. "Superalloys 1988", Seven Springs, USA (pub. The Metallurgical Society, 1988) p. 285.
[23] Glatzel U. and Feller-Kniepmeier M., *Scri. Metall.* **23** (1989) 1839.
[24] Ganghoffer J.F., Hazotte A., Denis S. and Simon A., *Scri. Metall. Mater.* **25** (1991) 2491.
[25] Hazotte A. and Denis S., Proc. ICRS4, Baltimore, USA (pub. the Society for Experimental Mechanics, 1994) p. 825.
[26] Hazotte A., Grosdidier T. and Denis S., *Scri. Metall. Mater.* **34** (1996) 601.
[27] Schmidt R. and Feller-Kniepmeier M., *Scri. Metall. Mater.* **26** (1992) 1919.
[28] Johnson W.C., *Metall. Trans. A* **18A** (1987) 233.